NUMERICAL SIMULATION OF DEMISTER EQUIPMENT FOR APPLICATION IN GRAVITATIONAL SEPARATORS

João Américo Aguirre Oliveira Jr., aguirre@esss.com.br
Clarissa Bergman Fonte, clarissa@esss.com.br
Carlos Eduardo Fontes, carlos.fontes@esss.com.br
Engineering Simulation and Scientific Software Ltda.

Carlos Alberto Capela Moraes, capela@petrobras.com.br
Petroleo Brasileiro S.A.

Abstract. *The present work is focused on the numerical simulation of an internal device for gravitational separator tanks to remove mist transported by gaseous streams, i.e. to minimize the so called* liquid carry over (LCO). *These internals are also known as demisters. These devices promote the recovery of liquid droplets that would be carried by the effluent gas stream avoiding both the waste of this material and problems downstream of the gravitational separator due to the presence of liquid in the gas stream. In this way the correct design and any improvement in the efficiency of the demister are very important. Currently the design of this kind of device is based mostly on empirical knowledge, generally using experimental correlations heavily simplified supplied by the main manufactures. In this kind of analysis the most of information acquired by the engineer is the overall efficiency value of the equipment operating in prescribed (ideal) conditions, i.e. the conditions for which the correlations were developed. Such ideal conditions, uniformity of the gas velocity, velocity limited in a narrow range, limited droplet sizes range, etc., are barely present inside of the separation equipment applied in the oil industry, mainly due to fluctuations in production conditions. The work developed here aims the formulation of a complete methodology for simulation of demisters by the use of computational fluid dynamics tools (CFD). This kind of simulation allows a detailed evaluation of the whole design. For this purpose the CFD package ANSYS Fluent version 6.3.26 is applied. In the numerical simulation at least two different fluid phases must be present: one Eulerian phase, the gas stream and; one Lagrangian phase, the mist (liquid droplets). In order to simulate the saturation and collected liquid dripping from the demister another Eulerian phase is necessary, the liquid collected. All these phases are strongly interacting, increasing the complexity of the numerical simulations. The demister is modeled as a thin surface inside of the gravitational separator. To calculate its efficiency based on local parameters (gas velocity, droplet diameter, equipment characteristics, etc.) additional models for boundary conditions were implemented in the CFD package . With the final methodology and additional models in hand, different configurations of demister inside gravitational separators are tested. The work is concluded with a final analysis of the results.*

Keywords: *demister equipment, numerical simulation, multiphase flows*

1. INTRODUCTION

Mist eliminator device, also called demister, is a commonly used internal device in the oil and gas industry and in other industrial segments to eliminate mist (very small disperse liquid droplets) from the gaseous streams. In the oil and gas industry one of the applications of this kind of equipment is as an internal device to gravitational separators in primary oil processing units, in order to minimize *liquid carry over* by effluent gas stream. These separators usually work with oil, water and gas mixtures (sometimes with sand also) from the risers. Allowing the mist to follow the gas stream, besides the economical losses, can produce liquid accumulation inside the gas piping, gas compressor problems and that can be a risk to the entire unit.

There are two main kinds of mist eliminators: the vane-pack and the wire-mesh demister. The main difference between these two types is the range of droplet diameter that each one can collect efficiently. The vane-pack type is designed to collect droplets bigger than the wire-mesh type. It is not uncommon to use both types in series, using the vane-pack to capture the bigger droplets and the wire-mesh to collect the smaller ones or using the wire-mesh to capture and coarsen small droplets and the vane-pack for the final collection. Figure 1 shows both types of demister.

In the design of mist eliminators as internal devices of separators, just average values of the operating conditions are applied. Values as average gas stream velocity, average droplet diameter and fluids physical properties are used. Additionally, some internal design "advices" are given in order to improve the incoming flow over the demister surface. Detailed analyses are very uncommon, although sometimes necessary for very critical applications.

The application of Computational Fluid Dynamics (CFD) in problems of the oil and gas industry has been a driving force to the development of multiphase flow formulations and methods and of entire CFD packages. The present group is focused on the application of CFD techniques to problems of primary oil processing in the oil and gas industry. This paper shows a particular application of Computational Fluid Dynamics in modeling of a demister equipment of the wire-mesh type using a multiphase simulation. The main objective of this work is to develop a methodology to simulate some

special cases where the precise design of demister equipment will be necessary. This is achieved using the ANSYS Fluent CFD package in a multiphase Euler-Lagrange simulation. The equipment itself is represented by an internal surface with a porous-jump type of condition and a User Defined Function (UDF) to determine the efficiency and collect the liquid droplets when they reach the demister.

Figure 1. Mist eliminator equipment, vane-pack type (left) and wire-mesh type (right).

1.1 Problem Description

The gravitational separators with mist eliminators will be treated as a main gas flow (gas with constant properties, since there is no significant variation of pressure and temperature inside of the separator), the Eulerian phase, and a secondary flow of liquid droplets, the Lagrangian phase.

In this kind of problem, it can be evaluated the influence of the disperse flow on the continuous flow properties (momentum, mass and temperature) by the calculation of a series of dimensionless parameters (Crowe, 2006). The application of these parameters in the operational conditions defined to this case shows that the dispersed phase has no significant influence on the continuous phase flow. Here, and in many other industrial applications, the dispersed phase flow can be solved in alter step after the solution of the continuous phase flow.

The mass flow of gas and liquid droplets were known, only the upper portion of the horizontal and vertical cylindrical separators that is available to the gas flow was simulated (the regions filled with liquid were discarded). Additional data will be available in Section 3.

2. PHYSICAL MODELING

As commented before, in many practical industrial applications either volume fraction (or loading) of the dispersed phase and droplets size are very small. This very small amount and small droplet size of dispersed phase let us consider that their effects on the continuous phase motion can be neglected without losing physical consistency or even accuracy. In these cases, the solution of the discrete phase motion can be performed after the solution of the continuous phase motion, in an serial fashion. This approach is known as "one-way coupling". This makes the numerical simulation of multiphase flows very cheap, since the main (continuous phase) flow can be computed as an steady-state single-phase flow and the discrete phase flow computed in a latter step using the Lagrangian approach.

The basic physical description and mathematical modeling of the continuous and discrete phases is given in the subsections below.

2.1 Continuous Phase Modeling

Since the "one-way coupling" approach can be applied, the continuous phase flow can be solved as a single-phase flow. The steady-state, isothermal and incompressible flow of a Newtonian fluid without any source terms or body forces is described by the conservation equations of mass and momentum. These equation are written, as shown in Fox and McDonald (2001), as Eq. (1) and Eq. (2).

$$\frac{\partial u_i}{\partial x_i} = 0 \tag{1}$$

Where x_i is the position and u_i is the continuous fluid (Eulerian) phase velocity in the direction i.

$$u_j \frac{\partial u_i}{\partial x_j} = -\frac{1}{\rho}\frac{\partial p}{\partial x_i} + \nu \frac{\partial}{\partial x_j}\left(\frac{\partial u_j}{\partial x_i} + \frac{\partial u_i}{\partial x_j}\right) \tag{2}$$

Where p is the static pressure, ρ is the continuous fluid phase density and ν is the kinematic viscosity of the continuous fluid.

These equations are solved in ANSYS Fluent using the Finite Volume Method. Complete discussions of the method can be found in the books of Patankar (1980), Versteeg and Malalasekera (2007) and Maliska (2004). No additional discussion will be presented here. Turbulence effects were accounted using the SST model as defined in Menter (1994).

2.2 Discrete Phase Modeling

In a Lagrangian frame, the motion of the discrete droplets is solved by tracking many parcels (particles representing small groups of droplets with the same characteristics) throughout the domain (Fluent, Inc., 2006). Equation (3) is used to calculate the droplet velocity at each solved position.

$$m_p \frac{dv_i}{dt} = \frac{1}{2}\rho C_D A \left|u_i - v_i\right|(u_i - v_i) + F_i \tag{3}$$

Here m_p is the mass of the droplet, t is the time, v_i is the discrete fluid (Lagrangian) phase velocity, F_i the sum of forces in the direction i (other than the drag force), C_D is the drag coefficient and A is the area of the droplet projected in the direction of the main flow. For a spherical droplet, Eq. (3) can be written as in Eq. (4).

$$\frac{dv_i}{dt} = \frac{18\mu}{\rho_p d_p^2}\frac{C_D Re}{24}\left|u_i - v_i\right|(u_i - v_i) + \frac{F_i}{m_p} \tag{4}$$

Where ρ_p is the discrete fluid phase density, d_p is the droplet diameter, μ is the continuous fluid phase viscosity, Re the relative Reynolds number. The relative Reynolds number between continuous and discrete phases is given by:

$$Re = \frac{\rho d_p \left|v_i - u_i\right|}{\mu} \tag{5}$$

The solution of the discrete fluid phase motion is obtained calculating the local velocity of a parcel at the current position using Eq. (4) and updating its position (using the calculated velocity and a reference time-step). These steps are repeated until the parcel leaves the domain or reaches the limit number of calculations. For the drag coefficient, there is a large number of correlations available, for example, in the books of Crowe (1998) and Crowe, Sommerfeld and Tsuji (2006). By analyzing the current case, due to the very small droplets size, it is very unlikely that these droplets will suffer any kind of deformation. Aware of this, a simple standard drag model for a spherical particle can be applied. The chosen model is the model from the work of Morsi and Alexander (1972), available in the ANSYS Fluent interface. This model defines the drag coefficient using the expression below.

$$C_D = a_1 + \frac{a_2}{Re} + \frac{a_3}{Re^2} \tag{6}$$

With the constants a_1, a_2 and a_3 defined according to the cited work.

The additional forces term can include many different physical phenomena, such as lift, virtual mass and thermophoretic forces. Crowe (1998) gives a physical description of these forces and some alternatives for mathematical modeling. Due to the configuration of the problem, the only additional force considered in the simulations was the turbulent dispersion force. In a practical point of view, the turbulent dispersion force adds a fluctuating velocity component to the continuous phase velocity used in the parcel movement calculations. This fluctuating component is based on the local turbulent properties (turbulent kinetic energy, turbulent kinetic energy dissipation rate, etc.). With this force active, two particle tracks started at the same point will not present identical trajectories. In order to have samples statistically meaningful, the analyst has to inject a larger number of parcels than without turbulent dispersion force. In cases where the "one-way coupling" can be applied this additional cost is not significant. Additional information on the definition of the turbulent dispersion force can be found in Dehbi (2008).

2.3 Equipment modeling

The modeling of demister equipment is usually done during the global design analysis using data provided by manufacturers. The expressions applied to calculate the equipment efficiency use only average values (average droplet diameter, average gas velocity, etc.) and return a global (average) efficiency. Although in the majority of the cases this approach is satisfactory, in some cases a more detailed data is necessary. For such cases very few works are found in the literature.

Many manufacturers use as a base point to equipment dimensioning the ideal velocity, u_{ideal}, of the gas stream, given by Eq. (7).

$$u_{ideal} = k\sqrt{\frac{(\rho_d - \rho)}{\rho}} \tag{7}$$

The constant k is a characteristic of the equipment chosen and ρ_d is the dispersed phase density. This velocity is called ideal because is the average gas stream velocity which gives the maximum average efficiency of the demister. Based on the information of one manufacturer product sheet (ACS Industries, Inc., 2004) and using some additional field information from a private communication from the Petrobras engineers (Moraes, 2009) the following expressions were developed to calculate the local demister efficiency.

$$k_I = \begin{cases} \dfrac{(\rho_d - \rho)\, u_n d_p^{2.0}}{9.0\mu D} & u_n \leq u_{ideal} \\ \dfrac{-(\rho_d - \rho)\, d_p^{2.0}\, (u_n - 3.0k u_{ideal})}{18.0\mu D} & u_n > u_{ideal} \end{cases} \tag{8}$$

Here k_I is an inertial parameter, which accounts for the effect of the droplet inertia in the collisions with the wire-mesh, u_n is the magnitude of the local gas stream velocity component normal to the demister surface and D is the wire diameter of the wire-mesh. This inertial parameter is used in Eq. (9) to obtain the collision efficiency parameter ϵ.

$$\epsilon = 1.0 - \left[\frac{1.09814}{1.0 + (0.74536 k_I)^{0.99030}} \right] \tag{9}$$

$$A' = \frac{0.67 A_w e}{\pi} \tag{10}$$

A' is the effective wire surface area available for collisions with the droplets, A_w is the equipment wire surface area density and e is the equipment thickness. Using the results from Eq. (8), Eq. (9) and Eq. (10), the local equipment efficiency, η, can be estimated by Eq. (11).

$$\eta = 100 - \left[\frac{100.0}{exp\,(\epsilon A')} \right] \tag{11}$$

The demister equipment head loss in the gas stream was defined using typical head loss values according to data from manufacturers (ACS Industries, Inc., 2004) by a porous medium approximation (Fluent, Inc., 2006) via the definition of a medium permeability, α, the pressure jump coefficient, C_2 and applying Eq. (12) to calculate the local head loss, Δp.

$$\Delta p = - \left(\frac{\mu}{\alpha} u_n + C_2 \frac{1}{2} \rho u_n^2 \right) e \tag{12}$$

Only the dry head loss was included in this definition, since almost no data is available on the dependency of the equipment head loss on the collected liquid saturation.

3. STUDY DEFINITION

Two separator tank geometries were initially defined for the study. One horizontal separator and one vertical separator. For each separator model two configurations of the demister device were studied (also horizontal and vertical). All the configurations respect the limitations cited by the manufacturers (ACS Industries, Inc., 2004). Figure 2 shows all the separator/demister configurations and the boundaries definition.

The temperature and pressure operational conditions and the fluids properties are shown in Tab. 1. For the liquid droplets diameters an experimental distribution from field measurements was used (Moraes, 2009) with droplet diameters ranging from $0.31[\mu m]$ to $301.68[\mu m]$.

The principal dimensions and flow rates of liquid and gas in each separator configuration are listed in Tab. 2. Once the demister is chosen, all the device data is specified by the manufacturer, the data for the model used in this case is given in Tab. 3.

The demister is modeled in the simulation using a porous-jump condition. The flow properties of the porous-medium were defined using Eq. (12) and the values in Tab 3. The collection of the droplets was defined using User Defined Functions inside ANSYS Fluent. These UDFs are executed each time a parcel collides with a surface element of the demister. When executed the UDF calculates the local efficiency, using Eq. (7), Eq. (8), Eq. (9), Eq. (10) and Eq. (11), and decides whether the parcel is collected or not. If the parcel is collected, information about the droplets diameter,
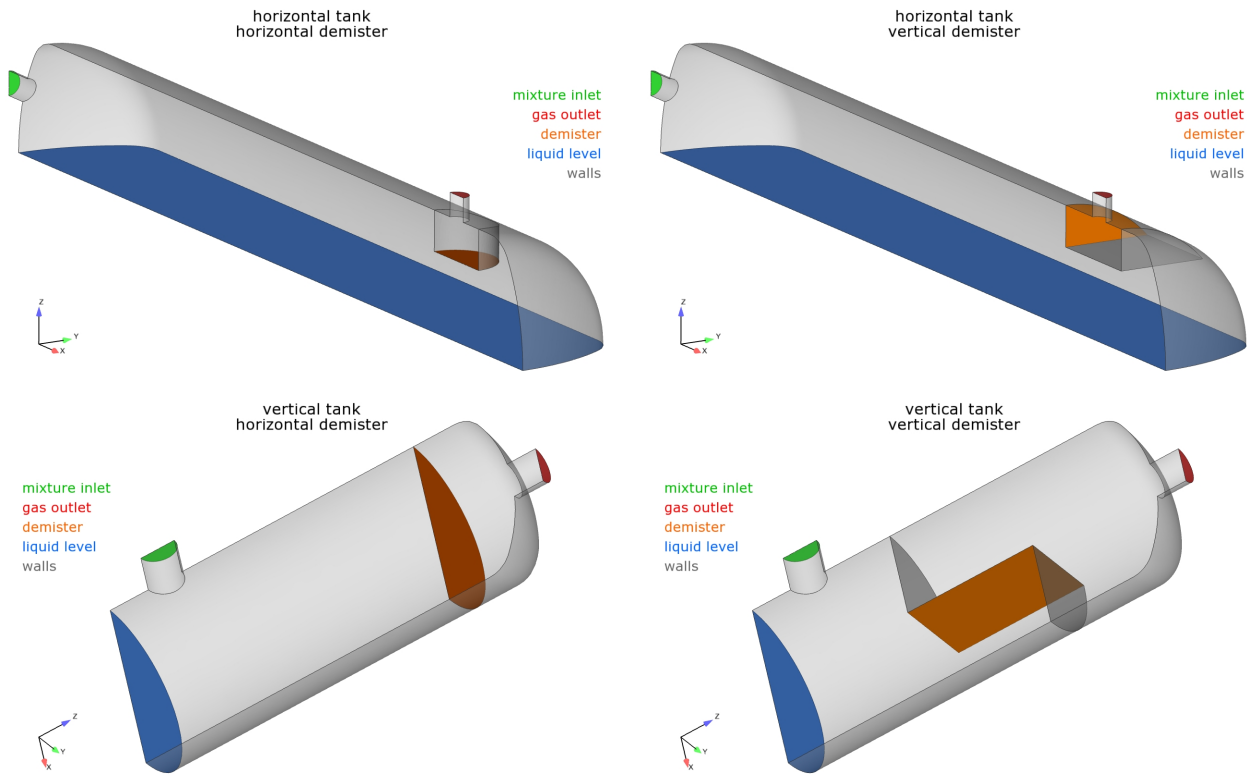
Figure 2. Geometries and boundaries definition for each tank/demister configuration.

Table 1. Operation conditions and fluids properties.

Operational conditions	
Temperature (T_0)	$343.15[K]$
Pressure (p_0)	$0.9[MPa]$
Gas properties	
Gas density (ρ)	$6.726[kg \cdot m^{-3}]$
Gas viscosity (μ)	$1.09 \cdot 10^{-5}[Pa \cdot s]$
Liquid properties	
Liquid density (ρ_d)	$800.0[kg \cdot m^{-3}]$
Liquid viscosity (μ_d)	$6.0 \cdot 10^{-3}[Pa \cdot s]$

Table 2. Separator configurations data.

Separator configuration	horizontal	vertical
Separator diameter (D_t)	$3.0[m]$	$1.45[m]$
Separator length (L_t)	$11.0[m]$	$4.5[m]$
Piping diameter (D_p)	$0.305[m]$	$0.305[m]$
Gas flow rate ($\dot{V}$)	$1.15[m^3 \cdot s^{-1}]$	$1.725[m^3 \cdot s^{-1}]$
Liquid mass flow rate ($\dot{m}_d$)	$6.81 \cdot 10^{-4}[kg \cdot s^{-1}]$	$1.02 \cdot 10^{-3}[kg \cdot s^{-1}]$
Demister hydraulic diameter (D_h)	$1.016[m]$	$1.45[m]$

droplets mass and droplets number from that parcel are stored to evaluate the average diameter, the total mass and the total number of particles collected locally at each demister surface element.

The boundary conditions imposed were: A velocity inlet at the mixture inlet surface; a pressure outlet at the gas outlet surface; a free slip wall at the liquid level surface; a no-slip wall at the walls surface group and; a porous-jump condition at the demister surface using the UDF to calculate the parcels fate. Due to the geometric symmetry over the center plane $x - z$, the actual geometry simulated was only half of the tanks, as shown in Fig. 2. For each separator/demister configuration, the main gas flow was solved and, using this solution, a set of droplets simulations was performed to

evaluate the final demister efficiency for each droplet diameter. A final simulation was performed using the experimental droplet distribution to verify the collection distribution on the demister surface. The results are presented and discussed in the next section.

Table 3. Demister equipment data.

Velocity constant (k)	$0.107[m \cdot s^{-1}]$	Area density (A)	$278.871[m^2]$
Medium permeability (α)	$2.61 \cdot 10^{-9}[m^2]$	Pressure coefficient (C_2)	$0.0[m^{-1}]$
Wire diameter (D)	$2.79 \cdot 10^{-4}[m]$	Equipment thickness (e)	$0.15[m]$

4. STUDY RESULTS

The simulations were executed as described before, solving the main flow of gas and, in a later step, running all the mist flow analysis using the same gas flow solution. The gas streamlines and the velocity distribution over the demister surface are shown in Fig. 3. In the case with the separator and the demister both in the horizontal position the flow over the demister surface is nearly uniform, the opposite can be seen in the vertical separator/vertical demister configuration, where the flow over the demister surface is very irregular. In both configurations one can see recirculation zones, suggesting that an additional internal device to homogenize the flow can be used to improve the flow distribution. A drastic case is the horizontal separator with vertical demister, where the major part of the tank is occupied by a big recirculation zone and there is a short circuit flow to the demister. The formation of this short-circuit flow has a negative influence over the demister efficiency because big droplets, that otherwise would fall to the liquid level surface, reach the demister inducing a faster saturation of the equipment.
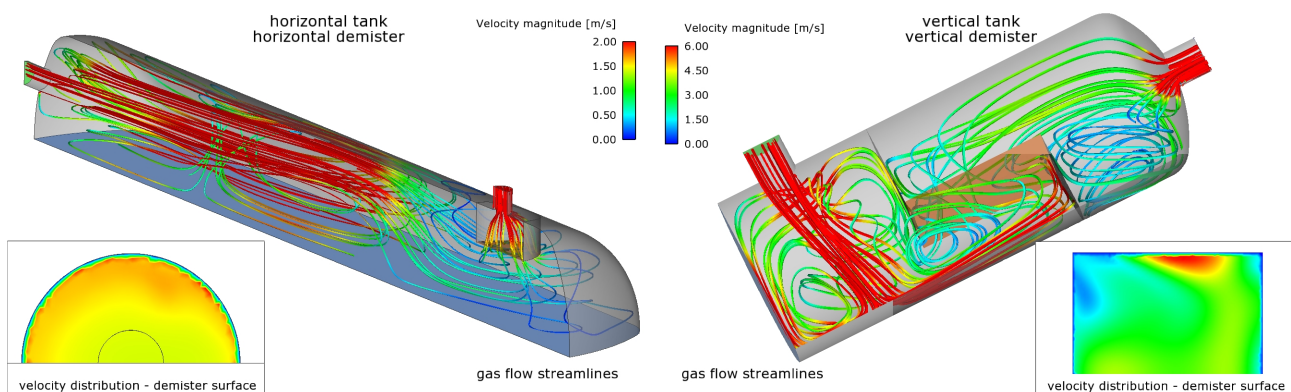

Figure 3. Gas flow streamlines and velocity distribution over the demister surface for the horizontal separator/horizontal demister and vertical separator/vertical demister configurations.

One of the main results from the simulations is the overall efficiency of the mist eliminators on each configuration. This data is shown in Fig. 4.

Figure 4 shows that the global efficiency of the mist eliminator equipment used in this study is not appropriate for this application. It was expected a low value of efficiency, since calculations using global averages (average gas velocity, average droplets diameter, etc.) and the equipment data have returned a value of $\eta = 62.4[\%]$. This low efficiency can be corrected by changing the equipment model to other with more appropriate characteristics (which, in practice, will change the values of k, A' and e).

As a complement to the global efficiency analysis, a detailed study of the efficiency variation with the droplets diameter was performed. The results of this study are shown in Fig. 5. One can see in this chart a typical efficiency curve, showing the reduction of the collection efficiency at the smaller diameters.

Figure 6 shows the distribution of collected droplets mass over the demister surfaces for all configurations. In this case the experimental size distribution was used. In all cases the mass collection distribution is very irregular. As commented before this can contribute to the poor efficiency of the devices, since some parts of the demister, those that receive more droplets, will saturate quickly, increasing the head loss and reducing the efficiency drastically.

5. CONCLUSIONS

The lack of efficiency in the demister model applied in this study is due to the main device characteristics, that are not ideal to collect such small droplets as we had in this case. Another demister model (even from the same manufacturer)
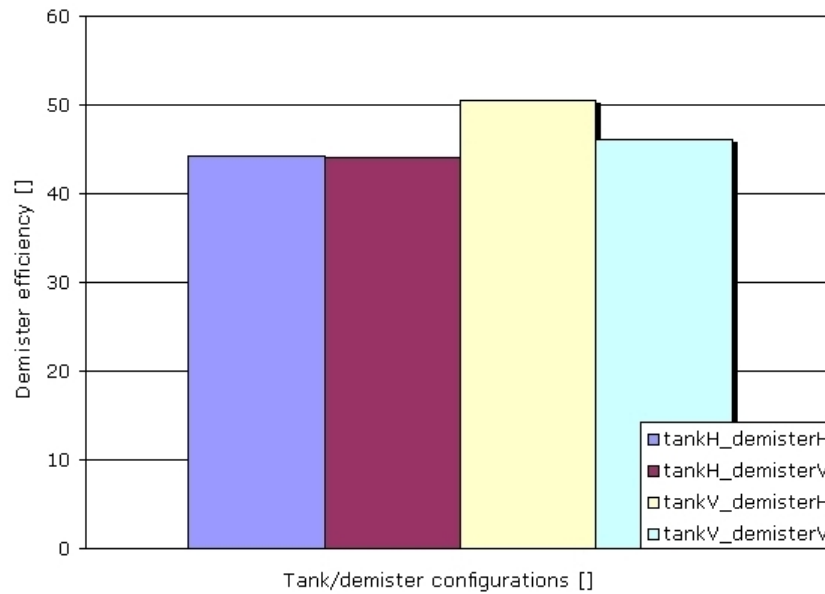
Figure 4. Global demister efficiency for each separator/demister configuration.
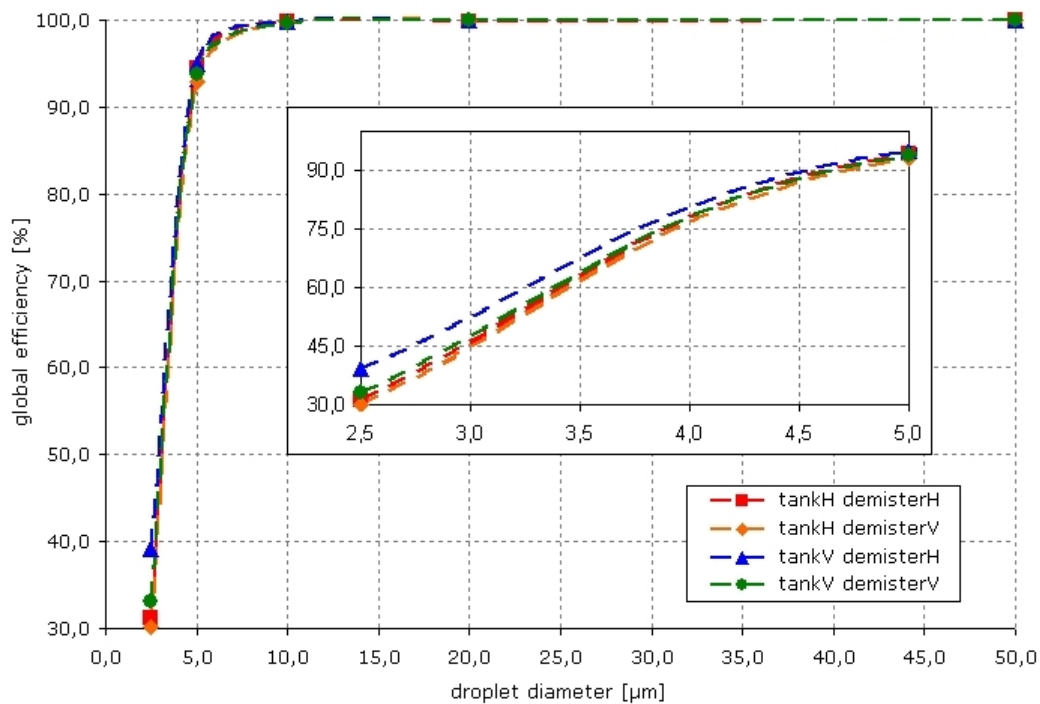

Figure 5. Demister efficiency variation with droplets diameter for each tank/demister configuration.

would be more appropriate. Other strong factor in this case was the non-uniform flow over the demister surfaces. This is shown in the details of Fig. 3 and Fig. 6. This non-uniformity will also have influence over the collected liquid removal from the device (as the liquid is collected in the wire-mesh it is conducted to some additional device and removed from the demister) making it harder to design the conductors.

The main objective of this work, to develop a methodology to simulate the flow of gas and mist and modelate the droplets collection over a demister equipment, was achieved. The simulation parameters and additional user routines (UDFs) required were defined. They can now be applied in real critical cases where detailed information about distribution of collection and efficiency data is necessary.
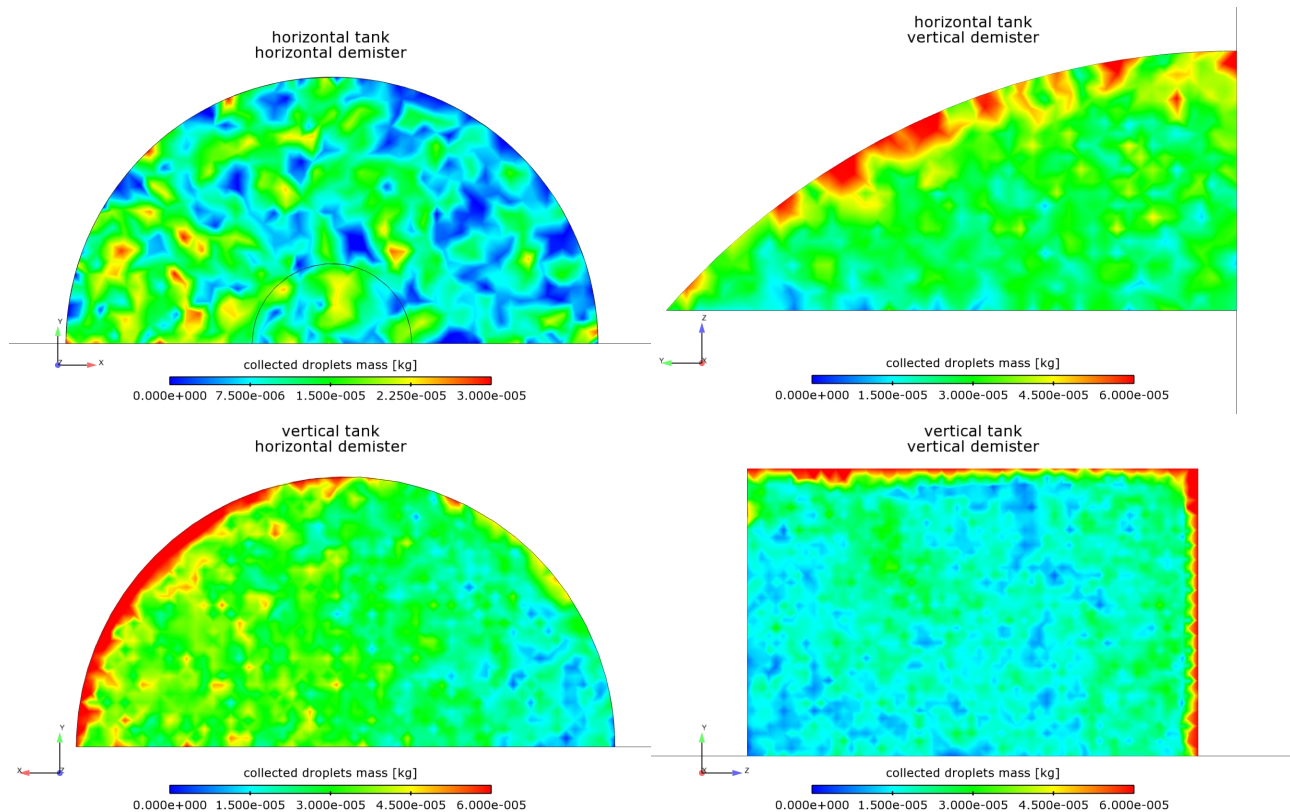
Figure 6. Distribution of collected droplets mass over the demister area for each separator/demister configuration.

5.1 Next steps

This work is still under development. The next step is to use the collected mass information to create a source term for a second Eulerian phase, the collected liquid. This will be helpful to verify the influence of the dripping liquid over the liquid surface (this dripping can perturb the separation of the liquids) and to design the devices to remove the collected liquid from the demister.

6. REFERENCES

ACS Industries, Inc., 2004, "The Engineered Mist Eliminator", www.acsseparations.com.

Crowe, C.T., 2006, "Multiphase Flow Handbook", CRC Press LLC, Boca Raton, USA, 1156 p.

Crowe, C.T., Sommerfeld, M. and Tsuji, Y., 1998, "Multiphase Flows with Droplets and Particles", CRC Press LLC, Boca Raton, USA, 471 p.

Dehbi, A., 2008, "Turbulent Particle Dispersion in Arbitrary Wall-Bounded Geometries: A Coupled CFD-Langevin-Equation Based Approach", International Journal of Mutiphase Flow, Vol.34, pp. 819-828.

Fluent, Inc., 2006, "Fluent 6.3 Documentation".

Fox, R.W. and McDonald, A.T., 2001, "Introdução à Mecânica dos Fluidos", 5 Edition, LTC Editora, Rio de Janeiro, 504 p.

Maliska, C.R., 2004, "Transferência de Calor e Mecânica dos Fluidos Computacional", 2 Edition, LTC, Rio de Janeiro, 472 p.

Menter, F.R., 1994, "Two-Equation Eddy-Viscosity Turbulence Models for Engineering Applications", AIAA Journal, Vol.32, No. 8, pp. 1598-1605.

Moraes, C.A.C., 2009, Private Communication.

Patankar, S.V., 1980, "Numerical Heat Transfer and Fluid Flow", Hemisphere, Washington, D.C., 214 p.

Versteeg, H.K. and Malalasekera, W., 2007, "An Introduction to Computational Fluid Dynamics: The Finite Volume Method", 2 Edition, Prentice Hall, New Jersey, 520 p.

7. RESPONSIBILITY NOTICE

The author(s) is (are) the only responsible for the printed material included in this paper